Silent memory engrams as the basis for retrograde amnesia

Dheeraj S. Roy[a,1], Shruti Muralidhar[a], Lillian M. Smith[a], and Susumu Tonegawa[a,b,c,2]

[a]RIKEN-Massachusetts Institute of Technology Center for Neural Circuit Genetics at the Picower Institute for Learning and Memory, Department of Biology and Department of Brain and Cognitive Sciences, Massachusetts Institute of Technology, Cambridge, MA 02139; [b]Howard Hughes Medical Institute, Massachusetts Institute of Technology, Cambridge, MA 02139; and [c]RIKEN Brain Science Institute, Wako-shi, Saitama 351-0198, Japan

Contributed by Susumu Tonegawa, September 28, 2017 (sent for review August 14, 2017; reviewed by Yadin Dudai and Sheena A. Josselyn)

Recent studies identified neuronal ensembles and circuits that hold specific memory information (memory engrams). Memory engrams are retained under protein synthesis inhibition-induced retrograde amnesia. These engram cells can be activated by optogenetic stimulation for full-fledged recall, but not by stimulation using natural recall cues (thus, amnesia). We call this state of engrams "silent engrams" and the cells bearing them "silent engram cells." The retention of memory information under amnesia suggests that the time-limited protein synthesis following learning is dispensable for memory storage, but may be necessary for effective memory retrieval processes. Here, we show that the full-fledged optogenetic recall persists at least 8 d after learning under protein synthesis inhibition-induced amnesia. This long-term retention of memory information correlates with equally persistent retention of functional engram cell-to-engram cell connectivity. Furthermore, inactivation of the connectivity of engram cell ensembles with its downstream counterparts, but not upstream ones, prevents optogenetic memory recall. Consistent with the previously reported lack of retention of augmented synaptic strength and reduced spine density in silent engram cells, optogenetic memory recall under amnesia is stimulation strength-dependent, with low-power stimulation eliciting only partial recall. Finally, the silent engram cells can be converted to active engram cells by overexpression of α-p-21–activated kinase 1, which increases spine density in engram cells. These results indicate that memory information is retained in a form of silent engram under protein synthesis inhibition-induced retrograde amnesia and support the hypothesis that memory is stored as the specific connectivity between engram cells.

memory | engram | hippocampus | episodic | amnesia

A memory engram is the enduring physical or chemical changes that occur in brain networks upon learning, representing the acquired memory information. Memory engrams are held by a set of neuronal ensembles that are activated by learning, and reactivation of these neurons gives rise to recall of the specific memory (1–3). A combination of immediate early genes, transgenics, and optogenetic techniques has recently provided the long-sought gain-of-function evidence for engram cells in the dentate gyrus of the hippocampus (4–6). This evidence has been complemented by loss-of-function evidence in the lateral amygdala (7, 8). Further studies identified and investigated memory engram cells in various brain areas under a variety of mnemonically relevant behavioral protocols (9–18). Furthermore, optogenetic manipulations of specific engram cells in vivo permitted unprecedented investigations of the relationship between memory representations and animal cognition or behaviors, allowing inception of a false memory (5), switching memory valence (19, 20), ameliorating depression-like behaviors (21), and restoring a memory impairment in early Alzheimer's mice (22).

Another important benefit of engram cell identification is that it permits investigation of the fundamental synaptic, cellular, and circuit mechanisms for encoding, consolidation, and retrieval of specific memories. The results of the initial characterization of hippocampal engram cells were consistent with the notion (23–25) that encoding results in rapid augmentation of synaptic strength and dendritic spine density and thereby contributes to the formation of memory (6). However, this study suggested that postlearning maintenance of increased synaptic strength and spine density by protein synthesis is not obligatory for memory storage. The study further suggested that memory retention is associated with the generation and maintenance of connectivity between multiple engram cell ensembles residing along an anatomical pathway.

Studies on the nature and dynamics of engrams, engram cells, and their connectivity, however, have just begun. In this study, we investigated several parameters of a specific set of engram cells from mice under retrograde amnesia due to postlearning inhibition of protein synthesis. This led to a concept of "silent memory engrams," which are susceptible to optogenetic recall but not natural recall cues.

Results

Long-Term Stability of Silent Memory Engrams in Retrograde Amnesia. We used memory engram cell identification and manipulation technology (4) to tag the hippocampal dentate gyrus (DG) component of a contextual fear memory engram with ChR2-eYFP. To disrupt cellular memory consolidation, we systemically injected the protein synthesis inhibitor anisomycin (26), or saline as a control, immediately after contextual fear conditioning (CFC). The specific dosage of anisomycin used in this study did not alter the activity-dependent synthesis of ChR2-eYFP

Significance

We previously discovered that memory is retrieved robustly from protein synthesis inhibitor-induced retrograde amnesia by optogenetic activation of engram cells. Connectivity of engram cells correlates with memory information storage under amnesia, even though these amnesic engram cells lack learning-induced augmented synaptic strength. We term this state of engrams as "silent engrams." The significance of this study is threefold: first, the silent state of the engram can last for a prolonged period (at least 8 d post encoding); second, connectivity between engram cell ensembles is causally linked to optogenetic recall and hence memory information storage; and third, there is a molecular genetic method to convert an engram from a silent state to an active state.

Author contributions: D.S.R. and S.T. designed research; D.S.R., S.M., and L.M.S. performed research; D.S.R., S.M., L.M.S., and S.T. analyzed data; and D.S.R. and S.T. wrote the paper.

Reviewers: Y.D., The Weizmann Institute of Science; and S.A.J., The Hospital for Sick Children.

The authors declare no conflict of interest.

[1]Present address: Stanley Center for Psychiatric Research, Broad Institute of Massachusetts Institute of Technology and Harvard, Cambridge, MA 02139.

[2]To whom correspondence should be addressed. Email: tonegawa@mit.edu.

in DG cells (Fig. 1 *A*–*C*), as demonstrated by comparable levels of engram labeling in saline and anisomycin-treated groups. We next examined the behavioral effect of optogenetically stimulating DG engram cells in anisomycin-treated mice 2, 5, and 8 d post-CFC training (Fig. 1*D*). Before engram cell labeling, habituation to context A with light-off and light-on epochs did not cause freezing behavior in naive mice of the presaline or preanisomycin groups (Fig. 1*E*). One day after training, the saline group displayed robust freezing behavior, whereas the anisomycin group showed significantly less freezing during cued recall (Fig. 1*F*). Two days after training, mice were placed into context A for a blue light stimulation (engram activation) test session. Consistent with our previous study (6), neither group showed freezing behavior during light-off epochs, but both groups froze significantly during light-on epochs (Fig. 1*G*, *Left*). To assay the conditioned response to natural recall cues, mice were again tested in context B 24 h after the blue light was turned off, and retrograde amnesia was observed in the anisomycin-treated group (Fig. 1*G*, *Right*).

Next, we investigated functional engram cell–engram cell connectivity between the upstream engram cell ensemble in DG and the downstream engram cell ensemble in hippocampal CA3 and, further downstream engram cell ensemble in the basolateral amygdala (BLA) by quantifying the overlap of engram cells and endogenous c-Fos$^+$ cells in the downstream sites that appear due to stimulation by recall cues (Fig. 1 *H* and *I*). Natural recall cues resulted in reduced c-Fos$^+$/mCherry$^+$ overlap in both CA3 and BLA of anisomycin mice, 2 d after training. However, DG engram cell activation by blue light in amnesic mice resulted in equivalent overlap as natural cue-induced recall and optogenetically induced recall in saline mice (Fig. 1*J*). Remarkably, the recovery from amnesia through direct light activation of anisomycin-treated DG engram cells and the preferential, protein synthesis-independent functional engram connectivity was observed both 5 d (Fig. 1 *K* and *L*) and 8 d (Fig. 1 *M* and *N*) after training. These data indicate that the connectivity of DG engram cells and the downstream CA3 and BLA engram cells is retained for as long as 8 d after training even in the anisomycin-treated animals (Fig. 1*O*). These results also reveal that memory engram cells can be at least of two different states: (*i*) the "silent" state that is not susceptible to natural recall cues for reactivation but can be reactivated by optogenetic stimulation and (*ii*) the active state that is susceptible to both natural and optogenetic stimuli.

Strong Engram Stimulation Is Necessary for Memory Recall Restoration in Amnesic Mice. Although silent memory engrams persist in mice under protein synthesis inhibitor-induced retrograde amnesia, these engram cells lack learning-induced synaptic strength (6), which is a characteristic of active, consolidated memory engram cells. We investigated the strength dependency of optogenetic stimuli in reactivating silent engram cells for recall in retrograde amnesia. For this purpose, we used three levels of blue laser power: 25, 50, and 75% (Fig. 2 *A* and *B*). Using ex vivo electrophysiology, the effect of the three levels of blue laser power on engram cell activation was validated (Fig. 2*C*). At 25% laser power, direct light activation of DG engram cells resulted in memory recall in saline mice, but not in anisomycin mice (Fig. 2*D*). Optogenetic activation of DG engram cells was comparable in saline and anisomycin mice, as demonstrated by the overlap between light-induced endogenous c-Fos$^+$ cells and ChR2-labeled engram cells (Fig. 2*E*, *Left*). Crucially, engram activation in amnesic mice at this laser power showed significantly reduced c-Fos$^+$/mCherry$^+$ overlap in downstream CA3 and BLA engram cells, compared with the overlap in saline mice (Fig. 2*E*, *Middle* and *Right*). In contrast, at 50% (Fig. 2 *F* and *G*) and 75% (Fig. 2 *H* and *I*) laser power, engram activation in amnesic mice resulted in memory recall and levels of downstream engram cell reactivation equivalent to those of saline mice. Together, these data indicate that stronger optogenetic stimulation is required for memory restoration in amnesic mice (Fig. 2*J*), reflecting the silent state of memory engrams under this condition.

Inactivation of the Connectivity with Downstream Engram Cell Ensembles Prevents Optogenetic Memory Recall. The correlation between long-term (at least 8 d after encoding) retention of memory and the connectivity between upstream and downstream engram cell ensembles (2, 6) (Fig. 1) under amnesia suggests that there is a causal link between these two phenomena. To test this possibility, we developed a viral approach using tetanus toxin light chain (TetTox) (27) to inactivate engram-specific connections. We first inactivated the upstream medial entorhinal cortex (MEC) to DG engram cell connections by injecting a virus mixture of AAV$_9$-c-fos-tTA (22) and AAV$_9$-TRE-GFP-TetTox into MEC, while simultaneously labeling DG engram cells with a mixture of AAV$_9$-c-fos-tTA and AAV$_9$-TRE-ChR2-mCherry (Fig. 3 *A*–*C*). We validated learning-dependent labeling of MEC neurons with TetTox and that engram labeling in MEC and DG was comparable between saline and anisomycin groups (Fig. 3*D*). As expected, in natural memory recall tests of the CFC paradigm (Fig. 3 *E* and *F*), anisomycin eYFP and anisomycin TetTox mice displayed retrograde amnesia. Importantly, the effect of TetTox expression in engram cells of the MEC was shown by reduced freezing in saline TetTox mice compared with saline eYFP mice (Fig. 3*F*, *Left*). We also observed decreased overlap of c-Fos$^+$/mCherry$^+$ DG engram cells following natural memory recall (Fig. 3*F*, *Right*) in saline TetTox mice compared with saline eYFP mice. Two days after training, although MEC-to-DG engram cell connections were inactivated, DG engram activation in both eYFP and TetTox groups of saline and amnesic mice resulted in memory recall (Fig. 3*G*) and downstream engram cell reactivation (Fig. 3*H*). By contrast, when downstream DG-to-CA3 engram cell connections were inactivated (Fig. 3 *I* and *J*), DG engram activation resulted in memory recall (Fig. 3*K*) as well as downstream engram cell reactivation (Fig. 3*L*) in saline and anisomycin eYFP groups, but not in the saline and anisomycin TetTox groups. Interestingly, the saline TetTox mice in which DG-to-CA3 connections were inactivated showed normal levels of natural memory recall. This probably indicates that the direct entorhinal cortex to hippocampal CA3 engram cell input is sufficient for memory recall even if DG-to-CA3 connections were inactivated (28). These experiments demonstrate that an inactivation of engram cell connectivity downstream, but not upstream, prevents light-induced memory recall.

Conversion of a Silent Engram to an Active Engram by PAK1 Overexpression. Active engram cells exhibit a learning-induced increase of dendritic spine density, which is lacking in silent engram cells (6, 22, 29). We investigated the spine density of engram cells in saline- and anisomycin-treated mice 2, 5, and 8 d post-CFC training. The anisomycin group showed reduced DG engram cell-specific spine density, compared with the saline group, across all three time points (Fig. 4 *A*–*C*). By tagging the hippocampal CA1 component of a contextual fear memory engram with ChR2-eYFP (Fig. 4 *D* and *E*), we found that anisomycin-treated CA1 engram cells showed reduced spine density compared with the saline-treated CA1 engram cells (Fig. 4 *F*–*H*). This finding is consistent with data from anisomycin-treated DG engram cells (6). We then hypothesized that the reversal of dendritic spine deficits in CA1 engram cells of anisomycin-treated mice may rescue long-term memory by natural recall cues. To investigate this possibility, we took advantage of previous findings that spine formation can be regulated by α-p-21–activated kinase 1 (PAK1) overexpression (30, 31). We developed an adeno-associated virus (AAV) approach for the

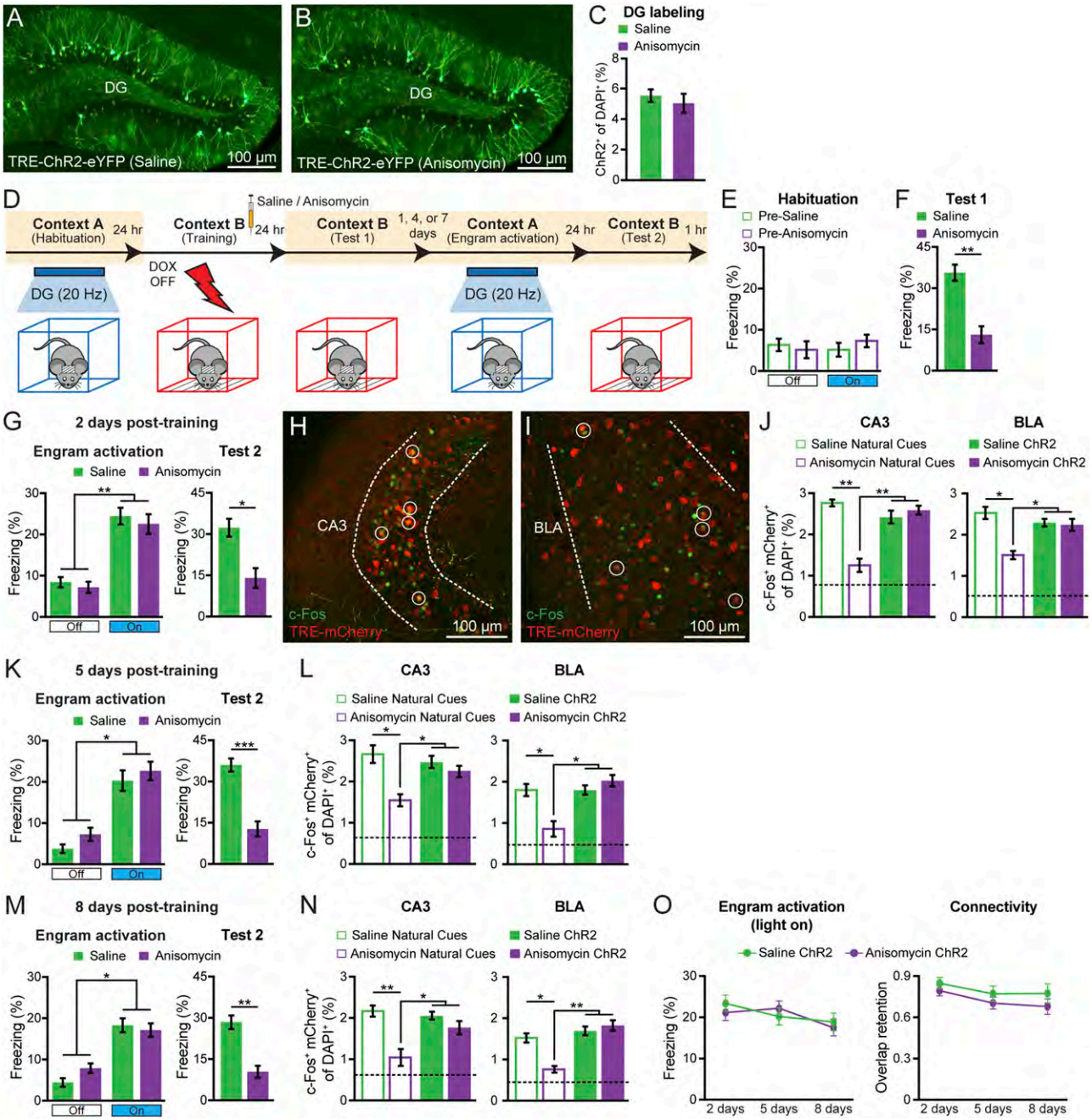

Fig. 1. Long-term stability of functional engram cell–engram cell connectivity in retrograde amnesia. (*A* and *B*) Hippocampal DG sections from c-fos-tTA mice injected with AAV_9-TRE-ChR2-eYFP virus, 24 h after saline (*A*) or anisomycin (*B*) injections. (*C*) Cell counts from saline ($n = 4$) and anisomycin ($n = 5$) groups. (*D*) Behavioral schedule. Beige shading signifies that mice were on a DOX diet, precluding ChR2-eYFP expression. Mice were habituated to optogenetic blue light stimulation at 20 Hz (~10–12 mW at patch cords). Mice were taken off DOX 24 h before CFC. Saline or anisomycin was injected immediately after training. One day after training, a natural recall test was performed (test 1). At 1, 4, or 7 d later, mice received an optogenetic recall (Engram activation) session. The next day a natural recall (test 2) session was performed. (*E*) Habituation. Presaline ($n = 10$) or preanisomycin ($n = 12$) groups. (*F*) Natural recall (test 1). (*G*) Optogenetic recall (*Left*) 2 d posttraining, and natural recall (test 2, *Right*). Saline ($n = 10$) and anisomycin ($n = 12$) groups. (*H* and *I*) Cell counting 2 d posttraining using c-fos-tTA mice with AAV_9-TRE-ChR2-eYFP injected into the DG and AAV_9-TRE-mCherry injected into both CA3 and BLA. Following natural recall or optogenetic recall, mice were perfused 1 h later. Images showing c-Fos expression (green), mCherry engram labeling (red), and c-Fos/mCherry overlap (white circles) in CA3 (*H*) and BLA (*I*). (*J*) c-Fos^+/$mCherry^+$ overlap in CA3 (*Left*) and BLA (*Right*) ($n = 4$ per group). Chance levels, indicated by black dashed lines, were estimated at 0.88 (CA3) and 0.49 (BLA). Anisomycin natural cues group data in CA3 and BLA are significantly greater than chance level (one-sample *t* tests against chance for CA3 and BLA, $P < 0.05$). Average mCherry labeling was 13.4% (of DAPI) in CA3 and 9.4% in BLA. Average cFos was 10.1% in CA3 and 7.6% in BLA except for the anisomycin natural recall group, which was 6.1%. (*K*) Optogenetic recall (*Left*) 5 d posttraining, and natural recall (test 2, *Right*). Saline ($n = 9$) and anisomycin ($n = 10$) groups. (*L*) Cell counting 5 d posttraining. c-Fos^+/$mCherry^+$ overlap ($n = 5$ per group). Chance at 0.79 (CA3) and 0.41 (BLA). (*M*) Optogenetic recall (*Left*) 8 d posttraining and natural recall (test 2, *Right*). Saline ($n = 9$) and anisomycin ($n = 8$) groups. (*N*) Cell counting 8 d posttraining. c-Fos^+/$mCherry^+$ overlap ($n = 3$ per group). Chance at 0.77 (CA3) and 0.43 (BLA). (*O*) Optogenetic recall (engram activation light-on epochs, *Left*) plotted for saline and anisomycin groups. Overlap retention (connectivity, *Right*) plotted as a ratio of ChR2-induced engram reactivation relative to natural recall-induced engram reactivation. Data shown for 2, 5, or 8 d posttraining. Data are presented as mean ± SEM. Unless specified, statistical comparisons are performed using unpaired *t* tests; $*P < 0.05$, $**P < 0.01$, $***P < 0.001$.

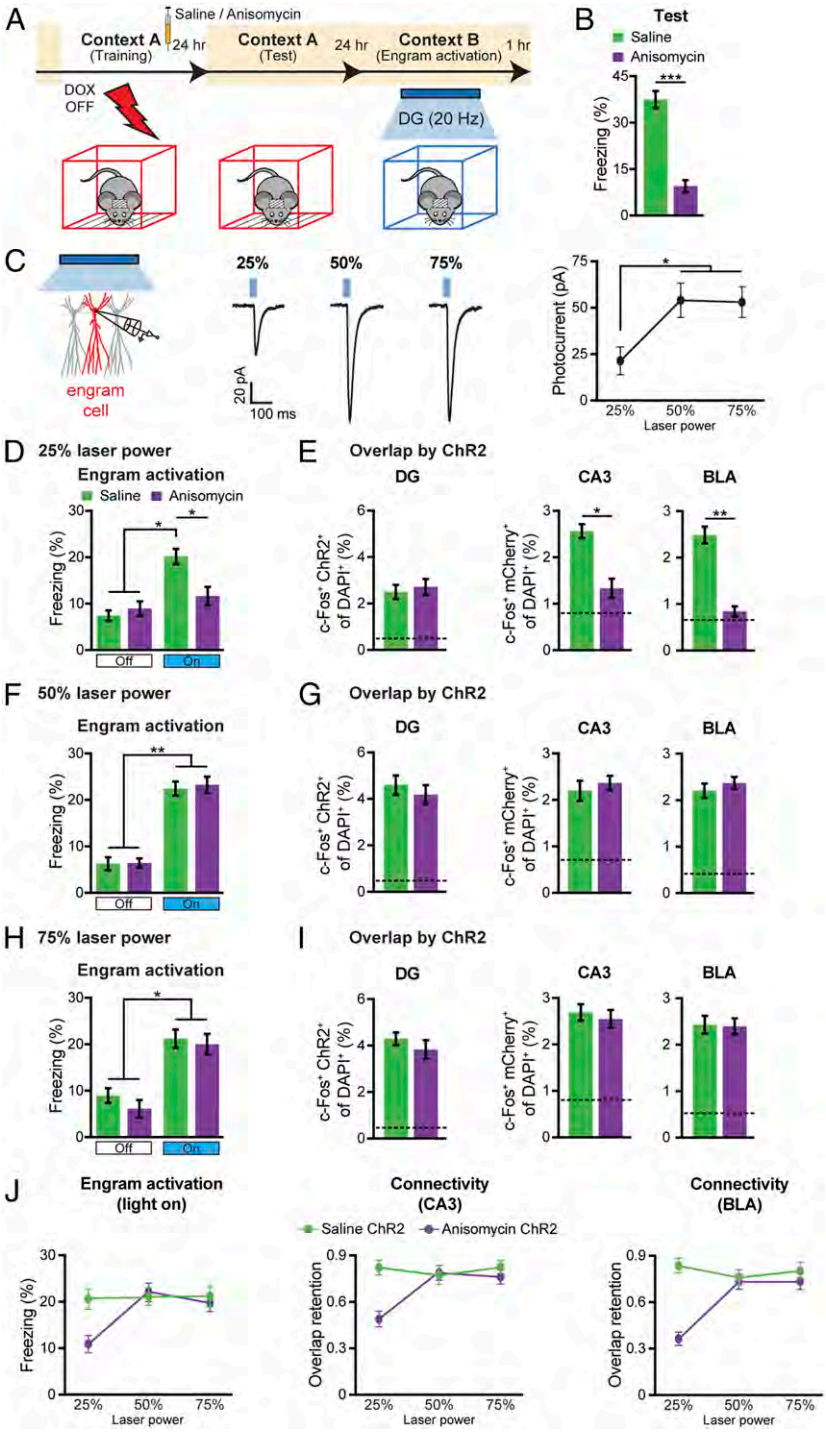

Fig. 2. Strong, but not weak, optogenetic stimulation of DG engram cells restores fear memory in retrograde amnesia. (*A*) Behavioral schedule. c-fos-tTA mice with AAV_9-TRE-ChR2-eYFP injected into the DG and AAV_9-TRE-mCherry injected into both CA3 and BLA were used. Mice were perfused 1 h postengram activation for cell-counting overlap. (*B*) Natural recall (test, $n = 9$ per group). (*C*) Ex vivo electrophysiological recordings of CA1 engram cells expressing AAV_9-TRE-ChR2-mCherry ($n = 6$), using 25% (~1.5–2.5 mW), 50% (~4–6 mW), and 75% (~7–9 mW) laser power (*Left*). Representative traces (*Middle*). Light-induced activation plotted as photocurrent (pA, *Right*). (*D*) Optogenetic recall using 25% laser. Significant freezing was observed in the saline group ($n = 9$), but not in the anisomycin group ($n = 8$). (*E*) Cell counting at 25% laser. c-Fos$^+$/ChR2$^+$ overlap in DG and c-Fos$^+$/mCherry$^+$ overlap in CA3 and BLA ($n = 5$ per group). Chance at 0.38 (DG), 0.89 (CA3), and 0.62 (BLA). In DG, average ChR2 labeling was 6.3% (of DAPI) and cFos was 4.4%. Average mCherry labeling was 12.7% in CA3 and 7.9% in BLA. Average cFos was 9.33% in CA3 for both groups, and 5.8% for saline or 3.92% for anisomycin in BLA. (*F*) Optogenetic recall using 50% laser. Significant freezing was observed in saline ($n = 10$) and anisomycin groups ($n = 10$). (*G*) Cell counting at 50% laser. c-Fos$^+$/ChR2$^+$ overlap in DG, c-Fos$^+$/mCherry$^+$ overlap in CA3 and BLA ($n = 4$ per group). Chance at 0.39 (DG), 0.82 (CA3), and 0.46 (BLA). (*H*) Optogenetic recall using 75% laser. Significant freezing was observed in saline ($n = 7$) and anisomycin groups ($n = 8$). (*I*) Cell counting at 75% laser. c-Fos$^+$/ChR2$^+$ overlap in DG, c-Fos$^+$/mCherry$^+$ overlap in CA3, and BLA ($n = 6$ per group). Chance at 0.37 (DG), 0.91 (CA3), and 0.51 (BLA). (*J*) Optogenetic recall (engram activation light-on epochs, *Left*). Overlap retention (connectivity, *Middle* and *Right*) in CA3 and BLA, plotted as a ratio of ChR2-induced engram cell reactivation relative to natural recall-induced engram reactivation levels. Data shown for 25, 50, or 75% laser power. Data are presented as mean ± SEM. Statistical comparisons are performed using unpaired *t* tests; $*P < 0.05$, $**P < 0.01$, $***P < 0.001$.

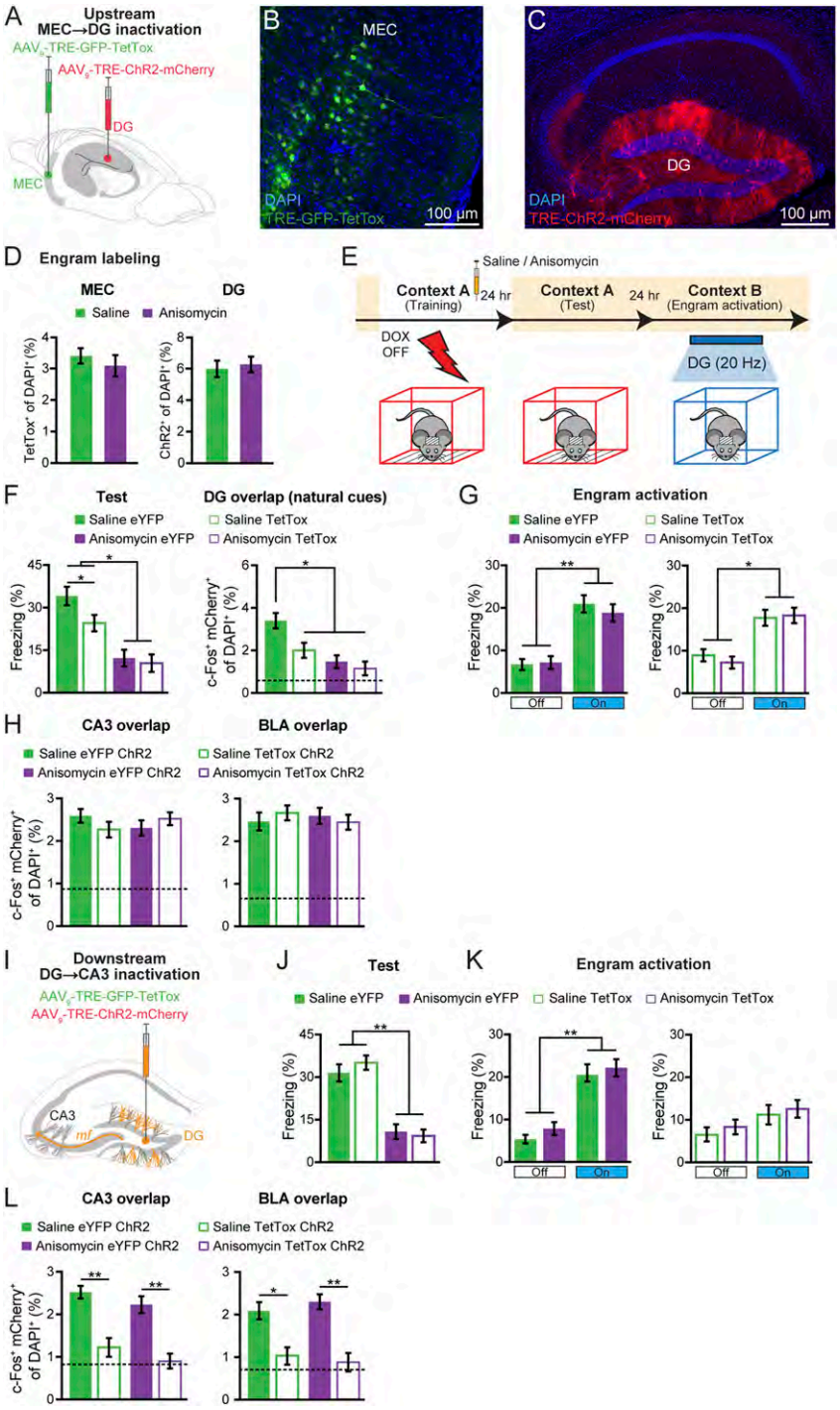

Fig. 3. Inactivation of engram cell connectivity downstream, but not upstream, prevents fear memory recall by optogenetic stimulation of DG engram cells in both control and retrograde amnesia. (*A*) Wild-type mice maintained on DOX were used. Virus mixture of AAV_9-c-fos-tTA/AAV_9-TRE-GFP-TetTox injected into the MEC to inactivate the upstream MEC-to-DG connection, and a mixture of AAV_9-c-fos-tTA/AAV_9-TRE-ChR2-mCherry into the DG, to label engram cells. (*B* and *C*) Sagittal sections of AAV_9-TRE-GFP-TetTox labeling in MEC (*B*) and AAV_9-TRE-ChR2-mCherry in DG (*C*). (*D*) GFP-TetTox counts from MEC and ChR2-mCherry counts from DG ($n = 3$ per group). (*E*) Behavioral schedule. In addition to TetTox mice, control mice injected with a virus mixture of AAV_9-c-fos-tTA/AAV_9-TRE-eYFP into MEC and a virus mixture of AAV_9-c-fos-tTA/AAV_9-TRE-ChR2-mCherry into the DG were also used. (*F*) Natural recall (test, *Left*, $n = 10$ per group). Saline-treated TetTox mice exhibited decreased freezing compared with saline eYFP. In a separate cohort, mice were perfused 1 h postnatural recall for overlap (*Right*). c-Fos$^+$/mCherry$^+$ overlap in DG ($n = 5$ per group). Chance at 0.42. Average cFos labeling was 3.87% (of DAPI) in saline eYFP, and 2.9% in other groups. (*G*) Optogenetic recall (~10–12 mW at patch cords). Significant freezing was observed in all groups ($n = 10$ per group). (*H*) c-Fos$^+$/mCherry$^+$ overlap in CA3 (*Left*) and BLA (*Right*) of eYFP or TetTox mice following ChR2-induced recall ($n = 4$ per group). Chance at 0.95 (CA3) and 0.59 (BLA). Average mCherry labeling was 12.6% in CA3 and 8.2% in BLA. Average cFos was 10.05% in CA3 and 7.1% in BLA. (*I*) To inactivate downstream DG to CA3, a mixture of AAV_9-c-fos-tTA/AAV_9-TRE-GFP-TetTox/AAV_9-TRE-ChR2-mCherry was injected into the DG. (*J*) Following the behavioral schedule in *E*, natural recall was performed (test, $n = 13$ per group). (*K*) Optogenetic recall (~10–12 mW at patch cords). Significant freezing was observed in both eYFP groups, but not in TetTox groups ($n = 12$ per group). (*L*) c-Fos$^+$/mCherry$^+$ overlap in CA3 (*Left*) and BLA (*Right*) of eYFP or TetTox mice following ChR2-induced recall ($n = 5$ per group). Chance at 0.91 (CA3) and 0.66 (BLA). Data are presented as mean ± SEM. Statistical comparisons are performed using unpaired *t* tests; $*P < 0.05$, $**P < 0.01$.

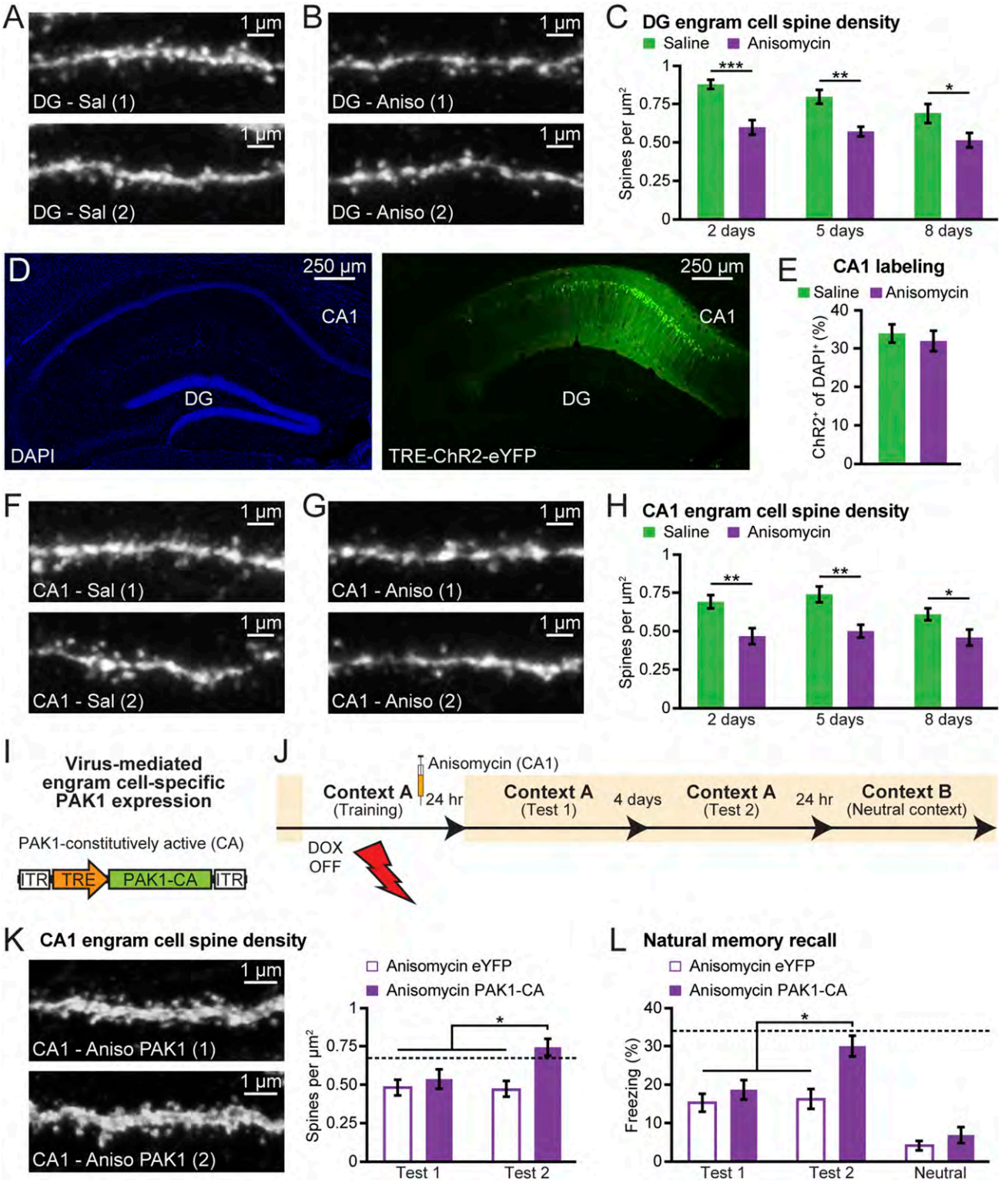

Fig. 4. Reversal of engram cell-specific spine deficits by PAK1 overexpression rescues natural memory recall in retrograde amnesia. (*A* and *B*) Dendritic spines from DG engram cells of saline (*A*) and anisomycin (*B*) groups. (*C*) Spine density post-CFC training from saline ($n = 7{,}045$ spines; $n = 7$ mice) and anisomycin ($n = 5{,}789$ spines; $n = 6$ mice). (*D*) Hippocampal CA1 sections from c-fos-tTA mice injected with AAV_9-TRE-ChR2-eYFP. DAPI (*Left*) and ChR2-eYFP (*Right*). (*E*) ChR2-eYFP counts from CA1 sections ($n = 4$ per group). (*F* and *G*) Dendritic spines from CA1 engram cells of saline (*F*) and anisomycin (*G*) groups. (*H*) Spine density post-CFC training from saline ($n = 5{,}122$ spines; $n = 6$ mice) and anisomycin ($n = 4{,}136$ spines, $n = 6$ mice). (*I*) Engram cell-specific PAK1 overexpression. (*J*) Behavioral schedule. (*K*) Dendritic spines from anisomycin-treated CA1 engram cells of the PAK1-CA group (*Left*). Spine density 1 d or 5 d post-CFC training from eYFP ($n = 3{,}895$ spines; $n = 5$ mice) and PAK1-CA ($n = 6{,}572$ spines; $n = 7$ mice) groups (*Right*). Black dashed line indicates saline mice spine density (0.72). (*L*) Natural recall 1 d (test 1) and 5 d (test 2) posttraining ($n = 15$ per group). Anisomycin PAK1-CA mice displayed increased freezing during test 2. Black dashed line indicates saline mice freezing level (34%). Data are presented as mean ± SEM. Statistical comparisons are performed using unpaired *t* tests; $^*P < 0.05$, $^{**}P < 0.01$, $^{***}P < 0.001$.

overexpression of constitutively active PAK1 (PAK1-CA) in a memory engram cell-specific manner (Fig. 4*I*). In mice that received anisomycin infusions only into hippocampal CA1, 5 d after training, PAK1-CA overexpression restored CA1 engram cell spine density to control levels (Fig. 4 *J* and *K*). Furthermore, this spine restoration in anisomycin-treated mice correlated with amelioration of long-term memory impairments observed during recall by natural cues (Fig. 4*L*, test 2), which was context-specific (Fig. 4*L*, neutral). These experiments identify a molecular genetic method to convert an engram from a silent state to an active state.

Discussion

An earlier study showed that, 1 d after training, synaptic strength and spine density in engram cells are augmented. However, an analysis of engram cells of mice that had received a blockade of posttraining protein synthesis indicated that memory retention did not depend on the maintenance of these changes in synaptic strength and spine density. Rather, the maintenance of learning-induced neuronal connectivity between engram cell ensembles correlated with memory retention (6). These findings support the idea that cellular consolidation is primarily for establishing memory retrievability rather than being an obligatory mechanism for storage of the representation per se (32, 33). In this study, we investigated this correlation more closely. First, we showed that the functional connectivity between engram cell ensembles lasted for a prolonged period after learning both in control mice and in anisomycin-treated mice. This was demonstrated in vivo by using the previously established overlap method of labeling upstream engram cells and downstream engram cells reactivated by activation of the former. Following the earlier demonstration of a significant overlap at 1 d after training (6), we have now shown that a similar degree of overlap is maintained at 5 d and 8 d after training between DG and CA3, as well as DG and BLA, engram cells. Furthermore, we confirmed that this long-term maintenance correlates with that of optogenetic memory recall. These results indicate that, once a specific pattern of connectivity between engram cell ensembles is established during learning, it is stable for at least a week, even in the absence of posttraining protein synthesis. Second, in this study we demonstrated that for optogenetic memory recall to take place by activation of an engram cell ensemble (DG), in either normal or anisomycin-treated mice, intact connectivity with a downstream engram cell ensemble (CA3) is crucial, whereas connectivity with an upstream engram cell ensemble (MEC) is not. These results provide causal evidence for the notion that engram cell ensemble connectivity is the basis for retained memory.

In anisomycin-treated animals, engram cells are in a silent state: the state in which memory information is retained and retrievable by optogenetic stimulation, but not by natural recall cues. The crucial feature of silent engram cells is the lack of augmented synaptic strength and spine density due to a posttraining blockade of protein synthesis. The efficiency of natural recall would be greatly influenced by these synaptic features, and below a certain threshold, effective recall will be blocked. In contrast, optogenetic recall is independent of synaptic strength and abundance, and hence it can be attained as long as a certain threshold of functional connectivity between engram cell ensembles is reached. However, since the engram cell connectivity would also depend on the synaptic strength and abundance, one would predict that functional engram cell connectivity would be weakened in anisomycin-treated animals, and hence optogenetic recall from these mice would depend on the strength of blue light. Our data in Fig. 2 confirmed this prediction: when the strength of blue light was reduced, both memory recall and functional engram cell connectivity were reduced. Furthermore, the crucial link between spine density, engram cell connectivity, and natural recall was demonstrated by restoration of full connectivity and natural recall by PAK1 overexpression in animals that received anisomycin infusions into hippocampal CA1.

Silent engrams are not a phenomenon specifically associated with retrograde amnesia. In a mouse model of early Alzheimer's disease, the hippocampal engrams are in a silent state that can be converted to an active state by repeated high-frequency stimulation of the engram cell synapses (22). In hippocampus-dependent episodic memory, engrams are formed rapidly on the day of learning not only in the hippocampus, but also in the prefrontal cortex (PFC). However, the PFC engrams are in a silent state and need to mature to acquire an active state, which takes many days and help from hippocampal engram cells. Conversely, the hippocampal engrams become silent as days go by (29). Furthermore, the longevity of social memory formed in ventral CA1 is relatively short-lasting—just several hours—but it continues to exist in a silent state for at least a few days (18). Thus, silent engrams are more routine than exceptional. Further studies on the properties of silent and active engrams and their mutual conversion would advance our understanding of the regulation of formation and retrieval of memory.

Materials and Methods

Animals. The c-fos-tTA transgenic mice were generated as described (4). The C57BL/6J wild-type mice were obtained from Jackson Laboratory. Mice had access to food and water ad libitum and were socially housed in numbers of two to five littermates until surgery. Following surgery, mice were singly housed. For behavioral experiments, all mice used for the experiments were male and 8–10 wk old at the time of surgery, had been raised on food containing 40 $mg{\cdot}kg^{-1}$ doxycycline (DOX) for at least 1 wk before surgery, and remained on DOX food for the remainder of the experiments except for the target engram labeling days. An identical procedure was used for virus-mediated (22) engram labeling experiments (Fig. 3) in which wild-type male mice were raised on DOX. All experiments were conducted in accordance with the National Institutes of Health guidelines and the Massachusetts Institute of Technology Department of Comparative Medicine and Committee on Animal Care.

Viral Constructs. The pAAV-TRE-GFP-TetTox and pAAV-TRE-PAK1-CA plasmids were constructed by cloning the GFP-TetTox and PAK1-CA (Addgene #12212) fragments into an AAV backbone containing the TRE promoter sequence (4). The pAAV-c-fos-tTA construct generation was done as described previously (22). The pAAV-TRE-ChR2-eYFP, pAAV-TRE-eYFP, pAAV-TRE-ChR2-mCherry, and pAAV-TRE-mCherry constructs were previously described (4, 6). AAV vectors were serotyped with AAV_9 coat proteins and packaged at the University of Massachusetts Medical School Gene Therapy Center and Vector Core or at Vigene Biosciences. Viral titers were 1.5×10^{13} genome copy (GC) mL^{-1} for AAV_9-c-fos-tTA, AAV_9-TRE-ChR2-eYFP, and AAV_9-TRE-eYFP, 1.2×10^{13} GC mL^{-1} for AAV_9-TRE-ChR2-mCherry, 2×10^{13} GC mL^{-1} for AAV_9-TRE-mCherry, and 3×10^{13} GC mL^{-1} for AAV_9-TRE-GFP-TetTox and AAV_9-TRE-PAK1-CA.

Surgery and Optic Fiber Implants. Mice were anesthetized with isoflurane or 500 $mg{\cdot}kg^{-1}$ avertin for stereotaxic injections, as described (22). Injections were targeted bilaterally to the DG [−2.0 mm anterior posterior (AP), ±1.3 mm medial lateral (ML), −1.9 mm dorsal ventral (DV)], MEC (−4.85 mm AP, ±3.36 mm ML, −2.75 mm DV), CA3 (−2.0 mm AP, ±2.3 mm ML, −2.2 mm DV), CA1 (−2.1 mm AP, ±1.5 mm ML, −1.4 mm DV), and BLA (−1.94 mm AP, ±3.1 mm ML, −4.65 mm DV). Injection volumes were 200 nL for DG and CA3, 300 nL for MEC and BLA, and 400 nL for CA1. A custom DG implant containing two optic fibers (200-mm core diameter; Doric Lenses) was used. As criteria, we included only mice with virus expression limited to the target regions.

Immunohistochemistry. Mice were perfused transcardially with 4% paraformaldehyde. Fifty-micrometer coronal slices were prepared using a vibratome. Immunostaining was performed as described (22). Antibodies used for staining were as follows: to stain for ChR2-eYFP, GFP-TetTox, or eYFP alone, slices were incubated with primary chicken anti-GFP (1:1,000; Life Technologies) and visualized using anti-chicken Alexa-488 (1:500). For ChR2-mCherry, or mCherry alone, slices were stained using primary rabbit anti-RFP (1:1,000; Rockland) and secondary anti-rabbit Alexa-555 (1:500). c-Fos was stained with rabbit anti–c-Fos (1:500; Calbiochem) and anti-rabbit Alexa-488 (1:300).

Cell Counting. To characterize the expression pattern of ChR2-eYFP, GFP-TetTox, eYFP, mCherry, c-Fos, and ChR2-mCherry in saline and anisomycin mice, the number of $eYFP^+$/GFP-$TetTox^+$/$mCherry^+$ neurons in five to seven coronal or sagittal slices per mouse (n = 3–6 mice per group) were counted. Coronal slices centered on coordinates covered by DG optic fiber implants and injection coordinates for CA3/CA1/BLA, and sagittal slices centered on injection coordinates for MEC were used. Semiautomated cell-counting analysis was performed using ImageJ software as described (22). $DAPI^+$ counts were approximated from five coronal/sagittal slices. All counting experiments were conducted blind to experimental group.

Spine Density Analysis. Engram cells were labeled using c-fos-tTA–driven synthesis of ChR2-eYFP or eYFP alone. The eYFP signal was amplified using immunohistochemistry procedures after which z-stacks were taken by confocal microscopy. For each mouse, 30–40 dendritic fragments of 10-μm length were quantified (n = 120–160 fragments per group). To measure spine density of DG engram cells, distal dendritic fragments in the middle-to-outer ML were selected. For CA1 engram cells, apical and basal dendritic fragments were selected. To compute spine density, the number of spines counted on each fragment was normalized by the cylindrical approximation of the surface of the fragment.

Behavior. Experiments were conducted as described (22). For natural recall sessions, data were quantified using FreezeFrame software. Light-induced freezing behavior was manually quantified. All behavior experiments were analyzed blind to the experimental group. For CFC, two distinct contexts were employed. The training context had grid floors, opaque triangular ceilings, red lighting, and 1% acetic acid scent. To disrupt cellular consolidation, 150 $mg{\cdot}kg^{-1}$ anisomycin, or an equivalent volume of saline, was delivered intraperitoneally immediately after CFC training. For CA1-specific experiments, anisomycin was delivered via cannulae (400 nL of a 150 $\mu g{\cdot}\mu L^{-1}$ stock). The engram activation context had perspex floors, transparent square ceilings, bright white lighting, and 0.25% benzaldehyde scent. Training consisted of three 0.75-mA shocks of 2 s duration in 5 min, and testing consisted of a 3-min context exposure. For light-induced freezing behavior, the chamber ceilings were customized to hold a rotary joint (Doric Lenses) connected to two 0.32-m patch cords. ChR2 was stimulated at 20 Hz (15-ms pulse width) using a 473-nm laser (10–15 mW) for the designated epochs, except in Fig. 2 where laser power was varied. Testing sessions were 12 min in duration, consisting of four 3-min epochs, with the first and third as light-off epochs, and the second and fourth as light-on epochs.

Ex Vivo Electrophysiology. Recordings were performed as described (6, 22). Briefly, 300-μm coronal slices containing dorsal hippocampus (CA1) were prepared. Whole-cell recordings in voltage-clamp mode were performed. Borosilicate glass pipettes were fabricated with resistances of 8–10 MΩ and filled with the following intracellular solution: 117 mM cesium methanesulfonate, 20 mM Hepes, 0.4 mM EGTA, 2.8 mM NaCl, 5 mM TEA-Cl, 4 mM Mg-ATP, 0.3 mM Na-GTP, and 0.5% biocytin (pH 7.25, osmolarity 290 mOsm). Optogenetics used a 460-nm LED light source. Light power on the sample was varied (25, 50, 75, 100%). Slices received a single pulse of light 2 ms in duration, every 5 s. Photocurrents (pA) were measured with the cell held at −70 mV.

ACKNOWLEDGMENTS. We thank S. Huang, S. LeBlanc, J. Martin, A. Arons, W. Yu, A. Hamalian, D. King, and C. Lovett for help with experiments; L. Brenner for proofreading; all members of the S.T. laboratory for their support; and Richard Palmiter for providing a tetanus toxin light-chain plasmid. This work was supported by the RIKEN Brain Science Institute, the Howard Hughes Medical Institute, and the JPB Foundation (S.T.).

1. Semon R (1904) *Die Mneme als erhaltendes Prinzip im Wechsel des organischen Geschehens* (Wilhelm Engelmann, Leipzig, Germany).
2. Tonegawa S, Liu X, Ramirez S, Redondo R (2015) Memory engram cells have come of age. *Neuron* 87:918–931.
3. Josselyn SA, Köhler S, Frankland PW (2015) Finding the engram. *Nat Rev Neurosci* 16: 521–534.
4. Liu X, et al. (2012) Optogenetic stimulation of a hippocampal engram activates fear memory recall. *Nature* 484:381–385.
5. Ramirez S, et al. (2013) Creating a false memory in the hippocampus. *Science* 341: 387–391.
6. Ryan TJ, Roy DS, Pignatelli M, Arons A, Tonegawa S (2015) Memory. Engram cells retain memory under retrograde amnesia. *Science* 348:1007–1013.
7. Han JH, et al. (2007) Neuronal competition and selection during memory formation. *Science* 316:457–460.
8. Han JH, et al. (2009) Selective erasure of a fear memory. *Science* 323:1492–1496.
9. Denny CA, et al. (2014) Hippocampal memory traces are differentially modulated by experience, time, and adult neurogenesis. *Neuron* 83:189–201.
10. Tanaka KZ, et al. (2014) Cortical representations are reinstated by the hippocampus during memory retrieval. *Neuron* 84:347–354.
11. Cowansage KK, et al. (2014) Direct reactivation of a coherent neocortical memory of context. *Neuron* 84:432–441.
12. Matsuo N (2015) Irreplaceability of neuronal ensembles after memory allocation. *Cell Rep* 11:351–357.
13. Trouche S, et al. (2016) Recoding a cocaine-place memory engram to a neutral engram in the hippocampus. *Nat Neurosci* 19:564–567.
14. Ye L, et al. (2016) Wiring and molecular features of prefrontal ensembles representing distinct experiences. *Cell* 165:1776–1788.
15. Rashid AJ, et al. (2016) Competition between engrams influences fear memory formation and recall. *Science* 353:383–387.
16. Yokose J, et al. (2017) Overlapping memory trace indispensable for linking, but not recalling, individual memories. *Science* 355:398–403.
17. Cai DJ, et al. (2016) A shared neural ensemble links distinct contextual memories encoded close in time. *Nature* 534:115–118.
18. Okuyama T, Kitamura T, Roy DS, Itohara S, Tonegawa S (2016) Ventral CA1 neurons store social memory. *Science* 353:1536–1541.
19. Redondo RL, et al. (2014) Bidirectional switch of the valence associated with a hippocampal contextual memory engram. *Nature* 513:426–430.
20. Kim J, Pignatelli M, Xu S, Itohara S, Tonegawa S (2016) Antagonistic negative and positive neurons of the basolateral amygdala. *Nat Neurosci* 19:1636–1646.
21. Ramirez S, et al. (2015) Activating positive memory engrams suppresses depression-like behaviour. *Nature* 522:335–339.
22. Roy DS, et al. (2016) Memory retrieval by activating engram cells in mouse models of early Alzheimer's disease. *Nature* 531:508–512.
23. Hebb D (1949) *The Organization of Behavior* (Wiley & Sons, New York).
24. Holtmaat A, Svoboda K (2009) Experience-dependent structural synaptic plasticity in the mammalian brain. *Nat Rev Neurosci* 10:647–658.
25. Hübener M, Bonhoeffer T (2010) Searching for engrams. *Neuron* 67:363–371.
26. Davis HP, Squire LR (1984) Protein synthesis and memory: A review. *Psychol Bull* 96: 518–559.
27. Campos CA, Bowen AJ, Schwartz MW, Palmiter RD (2016) Parabrachial CGRP neurons control meal termination. *Cell Metab* 23:811–820.
28. Bernier BE, et al. (2017) Dentate gyrus contributes to retrieval as well as encoding: Evidence from context fear conditioning, recall, and extinction. *J Neurosci* 37: 6359–6371.
29. Kitamura T, et al. (2017) Engrams and circuits crucial for systems consolidation of a memory. *Science* 356:73–78.
30. Zhang H, Webb DJ, Asmussen H, Niu S, Horwitz AF (2005) A GIT1/PIX/Rac/PAK signaling module regulates spine morphogenesis and synapse formation through MLC. *J Neurosci* 25:3379–3388.
31. Hayashi ML, et al. (2004) Altered cortical synaptic morphology and impaired memory consolidation in forebrain- specific dominant-negative PAK transgenic mice. *Neuron* 42:773–787.
32. Dudai Y (2004) The neurobiology of consolidations, or, how stable is the engram? *Annu Rev Psychol* 55:51–86.
33. Hardt O, Wang SH, Nader K (2009) Storage or retrieval deficit: The yin and yang of amnesia. *Learn Mem* 16:224–230.